

This article was downloaded by:

On: 27 January 2011

Access details: *Access Details: Free Access*

Publisher *Taylor & Francis*

Informa Ltd Registered in England and Wales Registered Number: 1072954 Registered office: Mortimer House, 37-41 Mortimer Street, London W1T 3JH, UK



Phosphorus, Sulfur, and Silicon and the Related Elements

Publication details, including instructions for authors and subscription information:

<http://www.informaworld.com/smpp/title~content=t713618290>

Zinc-Induced Fluorescence Enhancement of the 5,10-Porphodimethene-Type Thiophene-Containing Calixphyrins

Yoshihiro Matano^a; Masato Fujita^a; Tooru Miyajima^a; Hiroshi Imahori^{abc}

^a Department of Molecular Engineering, Graduate School of Engineering, Kyoto University, Kyoto, Japan ^b Institute for Integrated Cell-Material Sciences (iCeMS), Kyoto University, Kyoto, Japan ^c Fukui Institute for Fundamental Chemistry, Kyoto University, Kyoto, Japan

Online publication date: 27 May 2010

To cite this Article Matano, Yoshihiro, Fujita, Masato, Miyajima, Tooru and Imahori, Hiroshi (2010) 'Zinc-Induced Fluorescence Enhancement of the 5,10-Porphodimethene-Type Thiophene-Containing Calixphyrins', *Phosphorus, Sulfur, and Silicon and the Related Elements*, 185: 5, 1098 – 1107

To link to this Article: DOI: 10.1080/10426501003773431

URL: <http://dx.doi.org/10.1080/10426501003773431>

PLEASE SCROLL DOWN FOR ARTICLE

Full terms and conditions of use: <http://www.informaworld.com/terms-and-conditions-of-access.pdf>

This article may be used for research, teaching and private study purposes. Any substantial or systematic reproduction, re-distribution, re-selling, loan or sub-licensing, systematic supply or distribution in any form to anyone is expressly forbidden.

The publisher does not give any warranty express or implied or make any representation that the contents will be complete or accurate or up to date. The accuracy of any instructions, formulae and drug doses should be independently verified with primary sources. The publisher shall not be liable for any loss, actions, claims, proceedings, demand or costs or damages whatsoever or howsoever caused arising directly or indirectly in connection with or arising out of the use of this material.

ZINC-INDUCED FLUORESCENCE ENHANCEMENT OF THE 5,10-PORPHODIMETHENE-TYPE THIOPHENE-CONTAINING CALIXPHYRINS

Yoshihiro Matano,¹ Masato Fujita,¹ Tooru Miyajima,¹
and Hiroshi Imahori^{1–3}

¹Department of Molecular Engineering, Graduate School of Engineering,
Kyoto University, Kyoto, Japan

²Institute for Integrated Cell-Material Sciences (iCeMS), Kyoto University,
Kyoto, Japan

³Fukui Institute for Fundamental Chemistry, Kyoto University, Kyoto, Japan

The synthesis, structure, and electrochemical/optical properties of the zinc complexes of 5,10-porphodimethene-type thiophene-containing (S,N₃-) and phosphole-containing (P,N₃-) calixphyrins are reported. The S,N₃- and P,N₃-calixphyrin free bases react with zinc(II) salts to give the corresponding zinc complexes in good yields. The S,N₃-calixphyrin–ZnI complex adopts a distorted square pyramidal geometry, with the S and N atoms at the basal positions. The S,N₃-calixphyrin–ZnX complexes emit red fluorescence with fluorescent quantum yields up to 23%, whereas the P,N₃-calixphyrin–ZnCl complex is weakly fluorescent. Among the first-row transition metals (Fe²⁺, Cu²⁺, and Zn²⁺) examined, the chelation-enhanced fluorescence is observed specifically for the Zn²⁺ ion. These results indicate that the 5,10-porphodimethene-type S,N₃-hybrid calixphyrin is a promising turn-on fluorescent probe for Zn²⁺ sensing.

Keywords Calixphyrin; chelation; fluorescence; thiophene; zinc

INTRODUCTION

Calixphyrins¹ are a class of reduced porphyrin analogs involving both sp²- and sp³-hybridized bridging *meso* carbon atoms. According to the number of sp³-hybridized carbons, calixphyrins are divided to porphomethenes, porphodimethenes, and porphotrimethenes, all of which possess reasonably flexible frameworks as well as rather rigid π -conjugated networks. Due to this structural diversity, the calixphyrin family has attracted increasing attention in coordination chemistry and supramolecular chemistry.²

Received 6 December 2008; accepted 13 January 2009.

Dedicated to Professor Naomichi Furukawa on the occasion of his 70th birthday.

This work was supported by a Grant-in-Aid for Science Research on Priority Areas (No. 20036028, Synergy of Elements) from the Ministry of Education, Culture, Sports, Science and Technology, Japan. We thank Prof. Yoshifumi Kimura (Kyoto University), Dr. Kengo Suzuki (Hamamatsu Photonics K.K.), and Dr. Takahiro Sasamori (Kyoto University) for the measurements and analyses of fluorescence lifetimes, an absolute fluorescence quantum yield, and X-ray crystal structures of **5a**, respectively.

Address correspondence to Yoshihiro Matano, Department of Molecular Engineering, Graduate School of Engineering, Kyoto University, Nishikyo-ku, Kyoto 615-8510, Japan. E-mail: matano@sci.kyoto-u.ac.jp

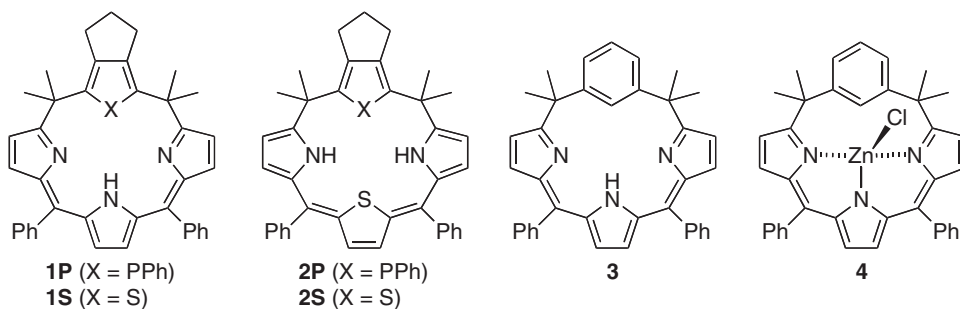


Figure 1 Core-modified 5,10-porphodimethenes reported by us³ and by Huang et al.⁵

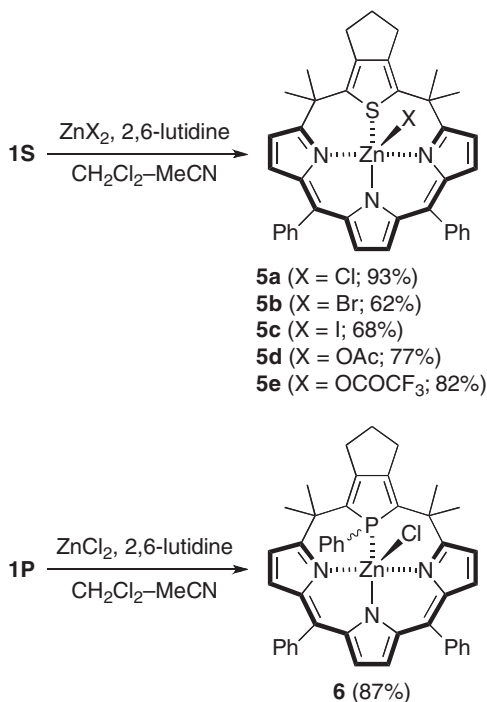
We have recently reported the first examples of the 5,10-porphodimethene-type hybrid calixphyrins containing phosphole and/or thiophene rings³ and disclosed the coordination properties of P,X,N₂-hybrid calixphyrins including **1P** and **2P** (Figure 1) with palladium, rhodium, and gold salts.^{3a,b} It is noteworthy that the oxidation state, charge, and catalytic activity at the metal center as well as the optical and electrochemical properties of the complexes vary significantly depending on the combination of the π -conjugated heterole units. In contrast to the P,X,N₂-hybrids **1P** and **2P**, however, the S,X,N₂-hybrids **1S** and **2S** did not produce complexes with the above transition metals, probably due to the weak coordinating property of the thiophene unit as compared to the phosphole unit.^{3c}

In 2008, Huang et al. reported that *m*-benziporphodimethene⁴ behaved as a long-wavelength Zn²⁺ specific chemosensor.⁵ Interestingly, compound **3** shows fluorescence switch-on upon Zn²⁺ binding with no apparent background fluorescence. Huang et al.'s findings represent the important role of the rigid and coplanar π -conjugated tripyrrin unit chelating to the central zinc ion of **4** in exhibiting strong emission. With this encouraging result in mind, we aimed to investigate the coordination chemistry of the thiophene- and phosphole-containing core-modified calixphyrins with Zn²⁺ ions and to reveal the effects of the core substituents on their light-emitting ability. In this article, we report the synthesis, structure, and electrochemical/optical properties of zinc complexes of the 5,10-porphodimethene-type S,N₃- and P,N₃-hybrid calixphyrins. It has been found that the efficiency of chelation-enhanced fluorescence is intrinsically dependent on the combination of heterole components of the calixphyrin platforms. The S,N₃-calixphyrin-zinc(II) complexes exhibit intense red fluorescence, whereas the P,N₃-calixphyrin-zinc(II) complex is weakly fluorescent.

RESULTS AND DISCUSSION

Thiophene- and phosphole-containing hybrid calixphyrins **1S**, **1P**, and **2S** were prepared according to the reported procedure.³ As depicted in Figure 1, the oxidation states and the available charges of the π -conjugated tripyrrin units of **1S** and **2S** differ from each other; **1S** is regarded as a monoanionic ligand with the 16 π network, whereas **2S** is a dianionic ligand with the 14 π network.⁶ The reaction of **1S** with ZnCl₂ in the presence of slight excess 2,6-lutidine in CH₂Cl₂-MeCN proceeded instantaneously at room temperature to give S,N₃-calixphyrin-ZnCl complex **5a** in 93% isolated yield. Similarly, **1S** underwent complexation with ZnBr₂, ZnI₂, Zn(OAc)₂, and Zn(OCOCF₃)₂ in the presence

of 2,6-lutidine to give the corresponding ZnX complexes **5b–e** ($X = \text{Br}, \text{I}, \text{OAc}, \text{OCOCF}_3$) in 62–82% isolated yields. When the S_2, N_2 -type free base **2S** was used in place of **1S**, no reaction took place with $\text{Zn}(\text{OAc})_2$. These results imply that the coordination behavior of the core-modified calixphyrins is deeply related to the components of the tripyrrin units. The P, N_3 -type free base **1P** reacted with ZnCl_2 in the presence of 2,6-lutidine to give P, N_3 -calixphyrin–ZnCl complex **6** in 87% yield (Scheme 1).



Scheme 1

All the zinc complexes **5a–e** and **6** are air-stable, dark blue or purple solids, and are soluble in common organic solvents such as CH_2Cl_2 , CHCl_3 , THF, toluene, and MeCN. The structures of **5a–e** and **6** were characterized by NMR spectroscopy and mass spectrometry. Complex **5a** displays one set of pyrrole- β protons at δ 6.19 (s, 2H), 6.65 (d, 2H), and 6.80 (d, 2H) as sharp peaks. Complexes **5b** and **5d** show their pyrrole- β protons at almost the same resonance frequencies as those of **5a**, implying that the axial anions (X) do not significantly influence the magnetic and electronic environments of the tripyrrin unit. On the other hand, **5c**, **5e**, and **6** exhibit two sets of pyrrole- β protons at slightly different frequencies in CDCl_3 , suggesting that two diastereomers are present in solution. It seems likely that in **5c**, **5e**, and **6**, the apical ligands coordinate to the zinc center from both sides of the macrocyclic planes (*vide infra*).⁷ In the mass spectra, fragment ions ($[\text{M}-X]^+$) were observed as the most intense peaks.

The structures of **5a** and **5c** were further elucidated by X-ray crystallography. Recrystallization of **5c** from CH_2Cl_2 –hexane afforded single crystals of one of the diastereomers. The top and side views of **5c** are depicted in Figure 2 with selected bond lengths and bond angles.⁸ The zinc center adopts a square pyramidal geometry coordinated by a sulfur

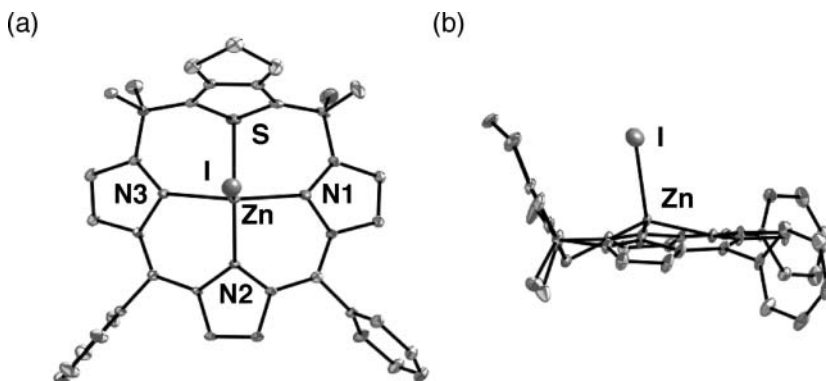


Figure 2 Top and side views of **5c** (30% probability ellipsoids). Hydrogen atoms and dichloromethane are omitted for clarity. Selected bond lengths (Å) and bond angles (deg): Zn–I, 2.4703(9); Zn–N(1), 2.162(5); Zn–N(2), 2.007(5); Zn–N(3), 2.170(5); Zn–S, 2.6724(16); S–Zn–N(1), 82.40(14); S–Zn–N(3), 78.97(14); N(2)–Zn–N(1), 90.4(2); N(2)–Zn–N(3), 91.73(19); I–Zn–N(1), 101.64(14); I–Zn–N(2), 110.95(16); I–Zn–N(3), 102.83(14).

atom and three nitrogen atoms at the basal positions. Due to the S-to-Zn coordination, the thiophene ring is inclined toward a mean tripyrrin plane with a dihedral angle of 67.4° , and the iodine atom is located on the same side of the thiophene-fused trimethylene unit with a relatively short Zn–I distance [2.4703(9) Å]. The Zn–N distances of **5c** [2.007(5)–2.170(5) Å] are comparable to those of Huang et al.'s ZnCl complex **4** [1.995(4)–2.130(4) Å]. The calixphyrin platform of **5c** displays a ruffled structure, and the zinc atom is displaced above the mean plane composed of the basal four heteroatoms by 0.61 Å with the sum of X–Zn–Y bond angles (X = S, N2; Y = N1, N3) of 343.5° . As a consequence, the π -conjugated tripyrrin unit in **5c** is slightly distorted with dihedral angles of 0.3 – 10.6° . The C–C bond alternation at the tripyrrin units observed for **5c** (Table I) reasonably explains a significant contribution of the canonical structures depicted in bold lines in Scheme 1.

Table I Selected bond lengths (Å) and dihedral angles (deg) of **5c**

a, a'	1.444(9), 1.448(9)	e, e'	1.419(8), 1.419(9)
b, b'	1.333(10), 1.356(9)	f, f'	1.423(8), 1.430(8)
c, c'	1.443(8), 1.445(9)	g	1.377(10)
d, d'	1.365(8), 1.386(8)		
c–d–e, c'–d'–e'	176.2(7), 169.4(6)		
d–e–f, d'–e'–f'	179.7(7), 176.3(7)		

Table II Reduction potentials and optical properties of **5a–e** and **6**^a

Complex	E_{red}^b	$\lambda_{\text{abs}}/\text{nm}^c$	$\log \varepsilon$	$\lambda_{\text{em}}/\text{nm}^d$	Φ_f
5a	−0.76	632	4.52	661	0.22 ^e
5b	−0.78	633	4.51	662	0.15 ^f
5c	−0.75	634	4.52	662	0.12 ^f
5d	−0.78	632	4.50	661	0.23 ^f
5e	−0.78	633	4.52	663	0.22 ^f
6	N. D. ^g	618	4.53	656	0.002 ^f

^aMeasured in CH₂Cl₂.^bReduction potentials vs. Fc[•]/Fc^{•+}.^cThe longest absorption maxima.^dExcited at 580 nm.^eAbsolute fluorescence quantum yield determined by a calibrated integrating sphere system.^fFluorescence quantum yield relative to **5a**.^gNot determined.

The observed structural features of **5a** are close to those of **5c**, although the quality of diffraction data for **5a** is not satisfactory. We have not succeeded in obtaining good single crystals of **6** so far.

To reveal apical-ligand effects on the electronic properties of the hybrid calixphyrin platforms, we measured electrochemical reduction processes of **5a–e** by cyclic voltammetry (CV) and differential pulse voltammetry (DPV). All the complexes showed reversible voltammograms in the CV measurements. As summarized in Table II, the electrochemical reduction occurred at almost the same potentials ($E_{\text{red}} = -0.75$ to -0.78 V vs. Fc[•]/Fc^{•+}; Fc[•] = decamethylferrocene, determined by DPV), suggesting that the apical ligands do not perturb the LUMO level significantly. The E_{red} values of **5a–e** are shifted to the positive side by comparison with that of the free base **1S** ($E_{\text{red}} = -0.93$ V vs. Fc[•]/Fc^{•+}). Presumably, the Lewis acidic Zn²⁺ center enhances the electron-accepting ability of the S,N₃-calixphyrin platform.

To disclose the optical properties of the S,N₃- and P,N₃-calixphyrin–zinc complexes, we measured UV-vis absorption and fluorescence spectra of **5a–e** and **6** in solution (Table II). The ZnCl complex **5a** displays intense, broad absorptions with absorption maxima at λ_{abs} 348, 585, and 632 nm in CH₂Cl₂ and at λ_{abs} 345, 580, and 624 nm in MeCN, due to π – π^* transitions of the tripyrrin unit. The zinc coordination induces a bathochromic shift of the lowest transition band by 92 nm ($\lambda_{\text{abs}} = 540$ nm for **1S** to $\lambda_{\text{abs}} = 632$ nm for **5a** in CH₂Cl₂). The spectral shape and extinction coefficients of **5b–e** are very close to those of **5a**, suggesting that the character of π – π^* transitions is little perturbed by the apical ligands in the S,N₃-calixphyrin–ZnX complexes. The P,N₃-calixphyrin–ZnCl complex **6** shows absorption bands at λ_{abs} 354 and 618 nm in CH₂Cl₂ and at λ_{abs} 351 and 612 nm in MeCN. The longest λ_{abs} values of **5a** and **6** in MeCN are appreciably blue-shifted as compared to those of **4** (λ_{abs} 350, 593, and 639 nm in MeCN), indicating that the coordination of the sp³-carbon-bridged heteroles influences on the electronic properties of the π -conjugated tripyrrin unit. The basal coordination of S (**5a**) and P (**6**) atoms to the zinc center may cause a deviation from planarity of the tripyrrin unit.

The most diagnostic spectral feature of **5a–e** is their highly fluorescent nature (Table II). In CH₂Cl₂, the ZnCl complex **5a** emits red fluorescence at $\lambda_{\text{em}} = 661$ nm ($\lambda_{\text{ex}} = 580$ nm) with a fluorescence quantum yield (Φ_f) of 0.22. In MeCN, the emission

is observed at 656 nm, which is blue-shifted by 16 nm compared to that observed for Huang et al.'s ZnCl complex **4** ($\lambda_{\text{em}} = 672$ nm in MeCN). The Φ_f value of **5a** is somewhat smaller than the reported value of **4** ($\Phi_f = 0.34$) but much larger than that of 5,10,15,20-tetraphenylporphyrinatozinc(II) ($\Phi_f = 0.033$).⁹ The Φ_f values of **5a–e** vary from 0.12 to 0.23 depending on the nature of apical ligands. Among the halides **5a–c**, the chloride **5a** shows the most intense fluorescence. In contrast to **5a–e**, the P,N₃-calixphyrin ZnCl complex **6** emits very weak fluorescence ($\Phi_f = 0.002$). These results represent an important role of the sp³-carbon-bridged heterole units in displaying chelation-induced fluorescence. It is worth mentioning that the S,N₃-hybrid free base **1S** is nonfluorescent. In this context, **1S** is regarded as a new fluorescence turn-on probe for Zn²⁺ ion.¹⁰

To get more insight into the photophysical properties, fluorescence lifetimes (τ_f) of **5a**, **5b**, and **5d** in CH₂Cl₂ were determined.¹¹ The fluorescence decays were well fit by the single exponential component, and τ_s values were determined to be 4.4 ns (**5a**), 3.0 ns (**5b**), and 4.3 ns (**5d**). Based on the observed Φ_f and τ_s values, fluorescence decay rate constants (k_f) of **5a**, **5b**, and **5d** were calculated to be $5.0 \times 10^7 \text{ s}^{-1}$, $5.0 \times 10^7 \text{ s}^{-1}$, and $5.3 \times 10^7 \text{ s}^{-1}$, respectively. These data imply that the difference in τ_s values among **5a**, **5b**, and **5d** is basically ascribable to the difference in rate constants of nonradiative processes from their S₁ states.

To evaluate the binding ability of **1S** as a fluorescent probe for sensing Zn²⁺ ion, spectrophotometric titration measurements were performed for the complexation of **1S** with ZnCl₂ or Zn(OAc)₂. As shown in Figure 3, adding ZnCl₂ (7.0×10^{-3} M in MeOH; 1–20 μL) into a red solution of **1S** (2.3×10^{-5} M in CH₂Cl₂; 3 mL) in the presence of 2,6-lutidine changed the spectral shape with isosbestic points at $\lambda = 430$ and 562 nm in the visible region. With increasing the concentration of Zn²⁺ ion, the fluorescence intensity increased. At a saturated condition (in the presence of 1.5 equiv of Zn²⁺ ion), the absorption and fluorescence spectra are identical to those independently observed for **5d**. Similar spectral changes were observed for the titration with Zn(OAc)₂. The 1:1 complexation between **1S** and Zn(OAc)₂ was further confirmed by a Job plot. To evaluate the coordinating ability of **1S** toward other transition metals, the titration measurements were also examined with Fe²⁺ and Cu²⁺ ions. Addition of a MeOH solution of FeCl₂ or CuCl₂ to a CH₂Cl₂ solution of **1S** (2.3×10^{-5} M) in the presence of 2,6-lutidine changed

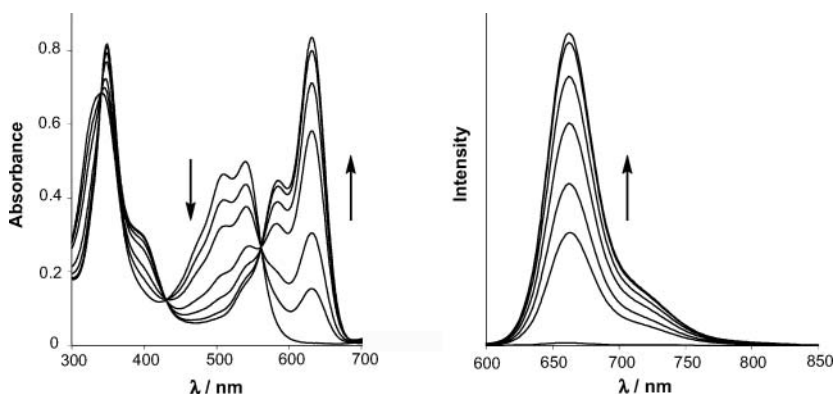


Figure 3 UV-vis absorption spectra (left) and fluorescence spectra (right, $\lambda_{\text{ex}} = 580$ nm) observed for the titration measurements of **1S** (2.3×10^{-5} M in CH₂Cl₂) with ZnCl₂ (7.0×10^{-3} M in MeOH) in the presence of 2,6-lutidine. [Zn²⁺] = 0, 0.3, 0.5, 0.8, 1.0, 1.2, 1.5 equiv vs. [**1S**].

its spectrum with isosbestic points at $\lambda = 438$ and 566 nm for Fe^{2+} and at $\lambda = 438$ and 569 nm for Cu^{2+} . The resulting spectra suggested the formation of S,N_3 -calixphyrin-iron ($\lambda_{\text{abs}} = 351$ and 645 nm) and -copper ($\lambda_{\text{abs}} = 356$, and 652 nm) complexes. In these complexations, however, almost no fluorescence ($\Phi_{\text{f}} < 0.001$) was detected, even at the saturated conditions, probably due to the paramagnetic effects. These results indicate that **1S** is an efficient fluorescence Zn^{2+} sensor emitting an intense red light. It should be mentioned again that **1P** does not show such a chelation-enhanced fluorescence. It is therefore likely that the core-modification of calixphyrin platforms impacts on the light-emitting ability of the Zn-coordinated tripyrrin π system.

In summary, we have revealed that the 5,10-porphodimethene-type S,N_3 - and P,N_3 -calixphyrins coordinate effectively to Zn^{2+} ions in solution. The S,N_3 -calixphyrin- ZnX complexes have been found to adopt a distorted square pyramidal geometry with S and N atoms at the basal positions and the anionic ligands at the apical position. Most importantly, the coordination of zinc(II) has proven to dramatically increase the fluorescence intensity of the S,N_3 -calixphyrin chromophores and to barely perturb the P,N_3 -calixphyrin chromophore. The efficiency of the chelation-enhanced fluorescence also depends on the transition metals coordinated at the core and is selective to Zn^{2+} among Fe^{2+} , Cu^{2+} , and Zn^{2+} ions. The present results demonstrate that the 5,10-porphodimethene-type S,N_3 -hybrid calixphyrin could be a promising turn-on fluorescent probe for Zn^{2+} sensing.

EXPERIMENTAL

^1H and $^{31}\text{P}\{^1\text{H}\}$ NMR spectra were recorded on a JEOL EX-400 or a JEOL AL300 spectrometer using CDCl_3 as a solvent. Chemical shifts are reported as the relative values vs. tetramethylsilane (^1H) or phosphoric acid (^{31}P). Matrix-assisted laser desorption/ionization (MALDI) time-of-flight mass spectra (TOF) were measured on a Shimadzu AXIMA-CFR spectrometer using α -cyano-4-hydroxycinnamic acid as a matrix. High-resolution mass spectra (HRMS) were recorded on a JEOL JMS-HX 110A spectrometer (FAB) using 3-nitrobenzylic alcohol as a matrix or a JEOL JMS-700 MStation spectrometer (EI). Electrochemical measurements (CV and DPV) were performed on a BAS 50 W electrochemical workstation using a glassy carbon working electrode, a platinum wire counter electrode, and an Ag/Ag^+ [0.01 M AgNO_3 , 0.1 M $n\text{-Bu}_4\text{NPF}_6$ (MeCN)] reference electrode. The potentials were calibrated with $\text{FeCp}^*/\text{FeCp}^{*2+}$ [$E_{\text{mid}} = -0.37$ V vs Ag/AgNO_3]. UV-vis absorption and steady-state fluorescence spectra were measured using a Perkin-Elmer Lambda 900 UV/vis/NIR spectrometer and a SPEX Fluoromax-3 spectrofluorometer, respectively. Spectroscopy grade CH_2Cl_2 and MeCN was used for the measurements of UV-visible absorption and fluorescence spectra. Free bases **1S**, **1P**, and **2S** were prepared according to the reported procedures.³ Dichloromethane was distilled from calcium hydride under inert atmosphere before use. Other chemicals and solvents were of reagent grade quality, purchased commercially and used without further purification. Thin-layer chromatography and flash column chromatography were performed with Alt. 5554 DC-Alufolien Kieselgel 60 F₂₅₄ (Merck) and Silica-gel 60N (Kanto Chemicals), respectively. All the reactions were performed under an argon atmosphere unless otherwise stated.

Synthesis of 5

2,6-Lutidine (ca. $10\ \mu\text{L}$) was added to a mixture of **1S** (15 mg, 0.026 mmol), ZnX_2 (0.031 mmol), CH_2Cl_2 (2 mL), and MeCN (3 mL), and the resulting blue solution was

stirred for 30 min at room temperature. The reaction mixture was then concentrated under reduced pressure to leave a solid residue, to which CH_2Cl_2 (10 mL) and water (10 mL) were added. The organic phase was separated, and the aqueous phase was extracted with CH_2Cl_2 until the blue color of the organic extracts disappeared. The combined organic extracts were dried over MgSO_4 and evaporated under reduced pressure to leave a solid residue, which was reprecipitated from cold hexane at low temperatures to afford $\text{S}_3\text{N}_3\text{-ZnX}$ complex **5** as a blue to purple solid in high purity. When **1P** was used as the free base, the $\text{P}_3\text{N}_3\text{-calixphyrin-ZnCl}$ complex **6** was obtained in 87% yield as a dark blue solid.

5a: Mp 244–245°C; ^1H NMR (CDCl_3 , 400 MHz) δ 1.72 (s, 6H; Me), 1.93 (s, 6H; Me), 2.26–2.33 (m, 1H; CH_2), 2.42–2.52 (m, 1H; CH_2), 2.70–2.89 (m, 4H; CH_2), 6.19 (s, 2H; pyrrole- β), 6.65 (d, 2H, $J = 4.4$ Hz; pyrrole- β), 6.80 (d, 2H, $J = 4.4$ Hz; pyrrole- β), 7.33–7.47 (m, 10H; Ph); UV-vis (CH_2Cl_2) λ_{abs} (ϵ): 348 (30800), 585 (17400), 632 (32900); HRMS (EI): Calcd for $\text{C}_{39}\text{H}_{34}\text{ClN}_3\text{SZn}$ (M^+), 675.1453; Found, 675.1454; Anal. Calcd for $\text{C}_{39}\text{H}_{34}\text{ClN}_3\text{SZn}\bullet(\text{CH}_2\text{Cl}_2)_{0.5}$: C, 65.88; H, 4.90; N, 5.84. Found: C, 66.06; H, 5.05; N, 5.84.

5b: Mp > 300°C; ^1H NMR (CDCl_3 , 400 MHz) δ 1.72 (s, 6H; Me), 1.94 (s, 6H; Me), 2.24–2.35 (m, 1H; CH_2), 2.42–2.52 (m, 1H; CH_2), 2.70–2.92 (m, 4H; CH_2), 6.21 (s, 2H; pyrrole- β), 6.65 (d, 2H, $J = 4.6$ Hz; pyrrole- β), 6.82 (d, 2H, $J = 4.6$ Hz; pyrrole- β), 7.30–7.47 (m, 10H; Ph); UV-vis (CH_2Cl_2) λ_{abs} (ϵ): 349 (31400), 586 (17300), 633 (32600); HRMS (FAB): Calcd for $\text{C}_{39}\text{H}_{34}\text{BrN}_3\text{SZn}$ (M^+), 719.0948; Found, 719.0923.

5c: This complex was obtained as a mixture of two diastereomers (**A/B** = 9/1). Mp > 300°C; ^1H NMR (diastereomer **A**: CDCl_3 , 400 MHz) δ 1.71 (s, 6H; Me), 1.94 (s, 6H; Me), 2.24–2.36 (m, 1H; CH_2), 2.40–2.56 (m, 1H; CH_2), 2.73–2.93 (m, 4H; CH_2), 6.23 (s, 2H; pyrrole- β), 6.65 (d, 2H, $J = 4.9$ Hz; pyrrole- β), 6.85 (d, 2H, $J = 4.9$ Hz; pyrrole- β), 7.30–7.50 (m, 10H; Ph); ^1H NMR (diastereomer **B**: CDCl_3 , 400 MHz) δ 1.71 (s, 6H; Me), 1.94 (s, 6H; Me), 2.24–2.36 (m, 1H; CH_2), 2.40–2.56 (m, 1H; CH_2), 2.73–2.93 (m, 4H; CH_2), 6.19 (s, 2H; pyrrole- β), 6.65 (d, 2H, $J = 4.6$ Hz; pyrrole- β), 6.80 (d, 2H, $J = 4.6$ Hz; pyrrole- β), 7.30–7.50 (m, 10H; Ph); UV-vis (CH_2Cl_2) λ_{abs} (ϵ): 350 (31500), 588 (17700), 634 (33300); MS (FAB) m/z 640 ($[\text{M}-\text{I}]^+$).

5d: Mp 173–174°C; ^1H NMR (CDCl_3 , 400 MHz) δ 1.57 (s, 3H; Me), 1.72 (s, 6H; Me), 1.93 (s, 6H; Me), 2.24–2.36 (m, 1H; CH_2), 2.42–2.52 (m, 1H; CH_2), 2.72–2.91 (m, 4H; CH_2), 6.19 (s, 2H; pyrrole- β), 6.65 (d, 2H, $J = 4.6$ Hz; pyrrole- β), 6.80 (d, 2H, $J = 4.6$ Hz; pyrrole- β), 7.33–7.50 (m, 10H; Ph); UV-vis (CH_2Cl_2) λ_{abs} (ϵ): 348 (31000), 586 (17000), 632 (31900); MS (FAB) m/z 640 ($[\text{M}-\text{OAc}]^+$).

5e: This complex was obtained as a mixture of two diastereomers (**A/B** = 2/1). Mp 209–210°C; ^1H NMR (diastereomer **A**: CDCl_3 , 400 MHz) δ 1.72 (s, 6H; Me), 1.93 (s, 6H; Me), 2.25–2.53 (m, 2H; CH_2), 2.66–2.92 (m, 4H; CH_2), 6.19 (s, 2H; pyrrole- β), 6.65 (d, 2H, $J = 4.6$ Hz; pyrrole- β), 6.80 (d, 2H, $J = 4.6$ Hz; pyrrole- β), 7.34–7.50 (m, 10H; Ph); ^1H NMR (diastereomer **B**: CDCl_3 , 400 MHz) δ 1.72 (s, 6H; Me), 1.90 (s, 6H; Me), 2.25–2.53 (m, 2H; CH_2), 2.66–2.92 (m, 4H; CH_2), 6.22 (s, 2H; pyrrole- β), 6.65 (d, 2H, $J = 4.6$ Hz; pyrrole- β), 6.82 (d, 2H, $J = 4.6$ Hz; pyrrole- β), 7.34–7.50 (m, 10H; Ph); UV-vis (CH_2Cl_2) λ_{abs} (ϵ): 349 (32300), 588 (17700), 633 (32800); HRMS (FAB): Calcd for $\text{C}_{41}\text{H}_{34}\text{O}_2\text{N}_3\text{F}_3\text{SZn}$ (M^+), 753.1615; Found, 753.1578.

6: This complex was obtained as a mixture of two diastereomers (**A/B** = 3/2). Mp > 300°C; ^1H NMR (diastereomer **A**: CDCl_3 , 400 MHz) δ 1.19 (s, 6H; Me), 1.73 (s, 6H; Me), 2.05–2.45 (m, 2H; CH_2), 2.62–2.95 (m, 4H; CH_2), 6.29 (s, 2H; pyrrole- β), 6.52 (d, 2H, $J = 4.6$ Hz; pyrrole- β), 6.84 (d, 2H, $J = 4.6$ Hz; pyrrole- β), 7.19–7.56 (m, 15H; Ph); ^1H NMR (diastereomer **B**: CDCl_3 , 400 MHz) δ 1.18 (s, 6H; Me), 1.85 (s, 6H; Me),

2.26–2.33 (m, 2H; CH₂), 2.62–2.95 (m, 4H; CH₂), 6.28 (s, 2H; pyrrole- β), 6.48 (d, 2H, J = 4.4 Hz; pyrrole- β), 6.72 (d, 2H, J = 4.4 Hz; pyrrole- β), 7.19–7.56 (m, 15H; Ph); ³¹P{¹H} NMR (diastereomer **A** and **B**: CDCl₃, 162MHz) δ 29.4 and 21.2; UV-vis (CH₂Cl₂) λ_{abs} (ϵ): 354 (30600), 618 (33900); MS (FAB) m/z 716 ([M–Cl]⁺).

X-Ray Crystal Crystallographic Analysis

Single crystals of **5a** and **5c** were grown from CH₂Cl₂–hexane at room temperature. All measurements were made on a Rigaku Saturn CCD area detector with graphite monochromated Mo–K α radiation. The structures were solved by direct methods¹² and expanded using Fourier techniques.¹³ Nonhydrogen atoms were refined anisotropically, and hydrogen atoms were refined using the rigid model. All calculations were performed using the CrystalStructure crystallographic software package¹⁴ except for refinement, which was performed using SHELXL-97.¹⁵ Although the crystallographic data for **5a** are not at the publishable level, its structure was confirmed by X-ray crystallography. CCDC No. 715502 for **5c** contains the supplementary crystallographic data for this article. These data can be obtained free of charge via the Cambridge Crystallographic Data Centre, 12 Union Road, Cambridge CB21EZ, UK (fax: (+44)1223–336–033; e-mail: deposit@ccdc.cam.ac.uk).

Fluorescence Lifetime Measurements of 5a, 5b, and 5d

The fluorescence lifetimes were measured in CH₂Cl₂ using a streak camera as a fluorescence detector. All samples were excited by the second harmonic output (400 nm) from the amplified Ti:Sapphire laser system.

Titration Measurements of 1S with Transition Metal Salts

A CH₂Cl₂ solution of **1S** (2.3×10^{-5} M; 3 mL) was charged in a quartz cuvette (pass length = 1 cm), and a MeOH solution of ZnCl₂ (7.0×10^{-3} M in MeOH) was added in portions (0.3, 0.5, 0.8, 1.0, 1.2, 1.5 equiv vs. [**1S**]). At each step, the absorption and fluorescence spectra were measured, and the results are shown in Figure 3. The titration measurements of **1S** with Zn(OAc)₂, FeCl₂, and CuCl₂ were examined according to a similar procedure. The incorporation of the respective metals was confirmed by MS spectrometry, although the resulting complexes were not isolated. The fragment ion peaks ([M–Cl]⁺) are as follows: m/z = 632 (for **1S**–Fe complex) and 639 (for **1S**–Cu complex).

REFERENCES

1. V. Král, J. L. Sessler, R. S. Zimmerman, D. Seidel, V. Lynch, and B. Andrioletti, *Angew. Chem., Int. Ed.*, **39**, 1055 (2000).
2. For example, see: (a) J. L. Sessler, R. S. Zimmerman, C. Bucher, V. Král, and B. Andrioletti, *Pure Appl. Chem.*, **73**, 1041 (2001); (b) B. Dolensky, J. Kroulík, V. Král, J. L. Sessler, H. Dvornáková, P. Bour, M. Bernátková, C. Bucher, and V. Lynch, *J. Am. Chem. Soc.*, **126**, 13714 (2004); (c) M. O. Senge, *Acc. Chem. Res.*, **38**, 733 (2005); (d) N. N. Sergeeva, Y. M. Shaker, E. M. Finnigan, T. McCabe, and M. O. Senge, *Tetrahedron*, **63**, 12454 (2007); (e) J.-M. Benech, L. Bonomo, E. Solari, R. Scopelliti, and C. Floriani, *Angew. Chem., Int. Ed.*, **38**, 1957 (1999); (f) H. Furuta, T. Ishizuka, A. Osuka, Y. Uwatoko, and Y. Ishikawa, *Angew. Chem., Int. Ed.*, **40**, 2323 (2001); (g) D.-H. Won, M. Toganoh, Y. Terada, S. Fukatsu, H. Uno, and H. Furuta, *Angew.*

- Chem., Int. Ed.*, **47**, 5438 (2008); (h) P. J. Chmielewski and L. Latos-Grażyński, *Coord. Chem. Rev.*, **249**, 2510 (2005); (i) M. Stepień and L. Latos-Grażyński, *Acc. Chem. Res.*, **38**, 88 (2005); (j) I. Gupta, R. Fröhlich, and M. Ravikanth, *Chem. Commun.*, 3726 (2006); (k) C. Bucher, C. H. Devillers, J.-C. Moutet, J. Pécaut, G. Royal, E. Saint-Aman, and F. Thomas, *Dalton Trans.*, 3620 (2005); (l) A. Y. O'Brien, J. P. McGann, and G. R. Geier III, *J. Org. Chem.*, **72**, 4084 (2007); (m) M. Bernátková, B. Andrioletti, V. Král, E. Rose, and J. Vaissermann, *J. Org. Chem.*, **69**, 8140 (2004), and references therein.
3. (a) Y. Matano, T. Miyajima, T. Nakabuchi, H. Imahori, N. Ochi, and S. Sakaki, *J. Am. Chem. Soc.*, **128**, 11760 (2006); (b) Y. Matano, T. Miyajima, N. Ochi, T. Nakabuchi, M. Shiro, Y. Nakao, S. Sakaki, and H. Imahori, *J. Am. Chem. Soc.*, **131**, 14123 (2009); (c) Y. Matano, T. Miyajima, N. Ochi, Y. Nakao, S. Sakaki, and H. Imahori, *J. Org. Chem.*, **73**, 5189 (2008).
 4. Latos-Grażyński and coworkers reported the first synthesis of *m*-benziporphodimethene and their coordination properties with Zn, Cd, Hg, and Ni salts. M. Stepień, L. Latos-Grażyński, L. Szterenberga, J. Panek, and Z. Latajka, *J. Am. Chem. Soc.*, **126**, 4566 (2004).
 5. C.-H. Huang, G.-F. Chang, A. Kumar, G.-F. Lin, L.-Y. Luo, W.-M. Ching, and E. W.-G. Diau, *Chem. Commun.*, 978 (2008).
 6. The count of π electrons is based on the number of formal C=C and C=N double bonds.
 7. In CD₃CN, only one set of peaks was observed for **5c**, **5e**, and **6**, suggesting that interconversion between the two diastereomers is rapid on the NMR time scale in the polar solvent.
 8. C₄₀H₃₆Cl₂IN₃SZn, MW = 853.95, monoclinic, *P*2₁/a, *a* = 19.6800(16) Å, *b* = 8.9482(5) Å, *c* = 22.4930(14) Å, β = 115.884(2)°, *V* = 3563.7(4) Å³, *Z* = 4, *D*_c = 1.592 g cm⁻³, 7656 obsd, 434 variables, *R*_w = 0.2519, *R* = 0.0936 (*I* > 2.00σ(*I*)), GOF = 1.134.
 9. P. G. Seybold and M. Gouterman, *J. Mol. Spectrosc.*, **31**, 1 (1969).
 10. For selected reviews on Zn²⁺ sensing, see: (a) A. P. de Silva, H. Q. N. Gunaratne, T. Gunnlaugsson, A. J. M. Huxley, C. P. McCoy, J. T. Rademacher, and T. E. Rice, *Chem. Rev.*, **97**, 1515 (1997); (b) P. Jiang and Z. Guo, *Coord. Chem. Rev.*, **248**, 205 (2004); (c) K. Kikuchi, K. Komatsu, and T. Nagano, *Curr. Opin. Chem. Biol.*, **8**, 182 (2004); (d) N. C. Lim, H. C. Freake, and C. Brueckner, *Chem. Eur. J.*, **11**, 38 (2005); (e) Z. Dai and J. W. Canary, *New J. Chem.*, **31**, 1708 (2007).
 11. To avoid uncertainty derived from two diastereomers, fluorescence lifetimes of **5c**, **5e**, and **6** are not discussed here.
 12. A. Altomare, G. Cascarano, C. Giacovazzo, A. Guagliardi, M. Burla, G. Polidori, and M. Camalli, *J. Appl. Cryst.*, **27**, 435 (1994).
 13. P. T. Admiraal, G. Beurskens, W. P. Bosman, R. de Gelder, R. Israel, and J. M. M. Smits, *The DIRDIF-99 Program System, Technical Report of the Crystallography Laboratory*, University of Nijmegen (1999), The Netherlands.
 14. CrystalStructure 3.8.2: Crystal Structure Analysis Package, Rigaku and Rigaku/MSC (2000–2006), The Woodlands, TX, USA.
 15. G. M. Sheldrick, *SHELXL-97*, University of Göttingen, Germany (1997).